Assessment of online monitoring strategies for measuring N2O emissions from full-scale wastewater treatment systems

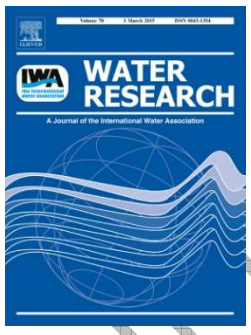

Ricardo Marques, Adrian Rodriguez-Caballero, Adrian Oehmen, Maite Pijuan

To appear in: *Water Research*

Received Date: 30 January 2016

Accepted Date: 20 April 2016

DOI: 10.1016/j.watres.2016.04.052

Elsevier Ltd.

Assessment of online monitoring strategies for measuring N_2O emissions from full-scale wastewater treatment systems

Ricardo Marques[a,b], A.Rodriguez-Caballero[b], Adrian Oehmen[a,*], Maite Pijuan[b]

[a]UCIBIO, REQUIMTE, Departamento de Química, Faculdade de Ciências e Tecnologia, Universidade Nova de Lisboa, Campus de Caparica, 2829-516 Caparica, Portugal

[b]ICRA, Institut Català de Recerca de l'Aigua, Parc Científic i Tecnològic de la Universitat de Girona, 17003 Girona, Spain

[*]Corresponding author: a.oehmen@fct.unl.pt; Phone: (+351) 212 948 571; Fax: (+351) 212 948 550

Abstract

Clark-Type nitrous oxide (N_2O) sensors are routinely used to measure dissolved N_2O concentrations in wastewater treatment plants (WWTPs), but have never before been applied to assess gas-phase N_2O emissions in full-scale WWTPs. In this study, a full-scale N_2O gas sensor was tested and validated for online gas measurements, and assessed with respect to its linearity, temperature dependence, signal saturation and drift prior to full-scale application. The sensor was linear at the concentrations tested (0 − 422.3, 0 – 50 and 0 − 10 ppmv N_2O) and had a linear response up to 2750 ppmv N_2O. An exponential correlation between temperature and sensor signal was described and predicted using a double exponential equation while the drift did not have a significant influence on the signal. The N_2O gas sensor was used for online N_2O monitoring in a full-scale sequencing batch reactor (SBR) treating domestic wastewater and results were compared with those obtained by a commercial online gas analyser. Emissions were successfully described by the sensor, being even more accurate than the values given by the commercial analyser at N_2O concentrations above 500 ppmv. Data from this gas N_2O sensor was also used to validate two models to predict N_2O emissions from dissolved N_2O

measurements, one based on oxygen transfer rate and the other based on superficial velocity of the gas bubble. Using the first model, predictions for N_2O emissions agreed by 98.7% with the measured by the gas sensor, while 87.0% similarity was obtained with the second model. This is the first study showing a reliable estimation of gas emissions based on dissolved N_2O online data in a full-scale wastewater treatment facility.

Keywords: Greenhouse gas (GHG) emissions; Wastewater Treatment Plants (WWTPs), Nitrous Oxide (N_2O); Online N_2O monitoring; Microsensors; Liquid-Gas mass transfer.

1. INTRODUCTION

Nitrous oxide (N_2O) is an important greenhouse gas with an approximate global warming potential 300-fold stronger than carbon dioxide (IPCC, 2013). Wastewater treatment plants (WWTP) have been shown to release significant amounts of N_2O and contribute to anthropogenic emissions, where it is produced during nitrification and denitrification (Ahn et al., 2010; Foley et al., 2010; Kampschreur et al., 2009). An emission factor as low as 0.5% of total nitrogen removed as N_2O can lead to emissions comparable to the indirect CO_2 emissions related with energy consumption in conventional biological nutrient removal WWTPs (de Haas and Hartley 2004), while in some cases N_2O emissions have been found to contribute over 80% of the total greenhouse gases emitted from WWTPs (Daelman et al., 2013a; Daelman et al., 2013b). Ahn et al., 2010 reported emission factors in the range of 0.01-1.8% and other studies have shown similar or even higher emission factors (Aboobakar et al., 2013; Daelman et al., 2015; Kampschreur et al., 2009; Rodriguez-Caballero et al., 2015; Ye et al., 2014). This high variability of emissions and the importance that N_2O has on the greenhouse gas budget of WWTPs highlights the need for assessing N_2O on an individual WWTP basis to be able to implement effective mitigation strategies suitable for each facility.

N_2O emissions from fully covered WWTPs can be determined with measurements of outlet N_2O gas concentrations and the total gas flow rate. However, most WWTPs are open-surface sludge systems, which are typically assessed using the floating chamber methodology, where the N_2O flux is captured (Law et al., 2012; Ye et al., 2014). The N_2O gas measurements can then be analysed off-line via e.g. gas chromatography (GC) by the use of grab samples or preferably via online commercial N_2O gas analysers, which can capture the variability of the emissions over time. However, these analysers require preconditioning of the gas sample (removing humidity and particles) and a minimum gas flow (0.5-1L/min depending on the analyser). This last step dilutes the concentration of N_2O, increasing uncertainty at the low N_2O concentration range (Marques et al., 2014). To overcome this limitation, a Clark-type N_2O microelectrode (Unisense Environment A/S) was adapted to measure N_2O in the gas phase, and was recently shown to be able to describe well the gas-phase N_2O emissions from lab-scale bioreactors (Marques et al., 2014). However, these sensors have not previously been applied to full-scale WWTPs, where the highly dynamic conditions inherent to WWTPs could have an important impact. Full-scale application is of high importance to validate the applicability of this novel methodology, in order to compare its effectiveness with conventional infrared online gas analysers.

Furthermore, the quantification of N_2O emissions based on liquid-phase N_2O measurements coupled with liquid-gas mass transfer estimations constitutes an alternative methodology for the assessment of N_2O emission factors in WWTPs. The N_2O that is produced and accumulated in the liquid phase can be transferred to the gas phase when N_2O is over-saturated, or stripped by aeration that facilitates the transfer of dissolved N_2O. The rate of the emissions in aerated and non-aerated zones can be estimated using volumetric mass transfer coefficients (K_La), liquid phase N_2O concentrations and the interphase transport between liquid and gas phases, relationships described by e.g. Schulthess and Gujer (1996) and Foley et al., (2010). Another alternative method to measure the dissolved N_2O concentration in the liquid phase was

developed by Mampaey et al. (2015), based on gas-phase measurements and mass transfer correlations. However, the use of liquid N_2O microsensors for continuous estimation of gas-phase N_2O emissions has not previously been reported, to the best of our knowledge, and could simplify the methodological procedure for assessing N_2O emissions.

In this study, the N_2O emissions of a full-scale WWTP treating domestic wastewater were measured via gas-phase microelectrodes and a conventional infrared online gas analyser, in order to assess the advantages/disadvantages with each monitoring approach. The impact of temperature as well as the sensor range and stability were firstly assessed for this purpose. Further, dissolved N_2O dynamics were also monitored with N_2O microsensors and were used to estimate N_2O emissions via mass transfer calculations. The aim of the work was to assess the applicability of microelectrodes for direct gas-phase N_2O measurements from a full-scale WWTP and to assess two different methodologies to estimate N_2O gas emissions from dissolved N_2O measurements.

2. MATERIALS AND METHODS

2.1. *Experimental setup for full-scale sensor calibration*

A Clark-Type N_2O gas sensor was used to measure N_2O emissions and a liquid N_2O microsensor was used for the liquid phase N_2O measurements in this study (Unisense Environment A/S, Denmark). Both sensors contained an internal reference and a guard cathode and before use, were connected to individual amplifier systems (Unisense Environment A/S, Denmark) and polarised overnight following manufacturer instructions (Unisense, 2014). The Clark-Type N_2O gas sensor was modified, as compared with the lab-scale version (Marques et al., 2014), to be more robust and prepared for handling shock impacts, and a temperature sensor was integrated within it to measure the variation of temperature in the gas phase along the measurement period (Fig. 1). To validate the N_2O concentration in the tests described below, a commercial N_2O online gas analyser (VA-3000, Horiba, Japan) was also used as well as a gas

chromatograph coupled to an electron capture detector (GC-ECD, Thermo Fisher Scientific, Trace GC Ultra, USA) with a column (TracePLOT TG-BOND Q, 30 m x 0.32 mm x 10 um). Three ranges of calibration curves (up to: 422.3 ppmv of N_2O, 50 ppmv of N_2O and 10 ppmv of N_2O) were tested according to Marques et al., (2014). Four different commercial N_2O gas mixtures were used in this experiment, 100% N_2O, 422.3, 104.3 and 83.7 ppmv N_2O (Linde, Spain). Mass flow controllers (Applikon Biotechnology, Netherlands) were used to achieve other desired N_2O concentrations using nitrogen as dilution gas. A 3 L vessel was used to perform the sensor calibration tests described below. The vessel was immersed in a water bath to control the temperature at the desired set-point. Temperature was measured with a temperature probe connected to an ez-control box (Applikon Biotechnology, Netherlands). The vessel was connected via gas tight tubing to a commercial N_2O analyser. Gas tight valves were used to seal the chamber after the volume of gas was fluxed to reach the desired N_2O concentration. A commercial hood (AC ′SCENT® Flux Hood, USA) was used to collect the gas from the full-scale wastewater reactor. The full-scale gas N_2O sensor was attached to the hood and the gas collected was directed to the commercial analyser via gas tubing.

2.2. *Experimental Procedure*

Several sets of tests were conducted to validate the most influential parameters on the sensor signal, as determined by Marques et al., (2014), including calibration curves at different N_2O concentrations, the sensor signal saturation, sensor drift and temperature dependence of the sensor were characterized prior to monitoring the wastewater treatment plant.

2.2.1. Full-scale gas sensor validation

The linearity of the sensor was tested with three different N_2O concentration ranges (High range: 0-422.3 ppmv N_2O; Medium range: 0-50 ppmv N_2O; Low range: 0-10 ppmv N_2O) using nitrogen as dilution gas. The methodology used was similar to that described by Marques et al.,

(2014). The sensor signal saturation was then tested with three different concentrations (1000, 2000 and 3000 ppmv of N_2O) to identify the upper N_2O detection limit of the sensor. The concentrations of the gas flow were simultaneously assessed by a commercial gas analyser and GC-ECD. The drift over time in the signal of the Clark-Type N_2O gas sensor was measured during 5h in a N_2O-free environment at a controlled temperature of 25 °C. The sensor drift was very low (0.016 mV/h) indicating that this sensor is suitable for long-term experiments with negligible influence on the target signal. Nevertheless, routine recalibration is recommended when measurements are performed for several days.

The temperature dependency was characterized using 3 different concentrations of N_2O. A zero current gas mixture, 25.5 ppmv of N_2O and 50.1 ppmv of N_2O. Calibration curves were performed within the range of 15-33 °C. To describe the influence of temperature on the sensor signal, a double exponential equation was used as described by Jenni et al., (2012) and Marques et al., (2014) (Equation 1):

$$S_{N_2O}(T, C) = a_1 \times e^{b_1 T} + a_2 \times C \times e^{b_2 T} \qquad (1)$$

where T is the temperature and C the concentration measured by the sensor, where a_i and b_i are the fitting parameters.

2.2.2. Full-scale liquid sensor and online commercial analyser calibration

The full-scale liquid sensor was calibrated according to the instructions present in the Unisense N_2O sensor manual. Briefly, the sensor was connected to an amplifier and polarized overnight following manufacturer instructions. A saturated solution with N_2O was obtained thought bubbling, at a flow rate of 5L/min, 100% N_2O during 5 minutes. A three-point calibration was obtained by adding twice 0.1 mL to 100 mL of free N_2O water. The online commercial analyser (VA-3000, Horiba, Japan) was calibrated with nitrogen gas free of N_2O to obtain a zero N_2O

157 calibration point and with a gas mixture of 422.3 ppmv of N_2O to perform a two-point
158 calibration curve. Both systems were calibrated before and after monitoring the WWTP.
159
160 *2.2.3. Full-scale monitoring tests*
161 N_2O emission dynamics were monitored online at a domestic WWTP of 48000 population
162 equivalents (P.E) (WWTP of La Roca del Vallès, Barcelona, Spain) in order to validate the full-
163 scale N_2O measurements from the gas sensor with a commercial analyser, and also with a liquid
164 phase N_2O sensor (Fig. 1 A,B). The plant consists of four identical SBRs with an operational
165 volume of 4684.2 m^3 each that were operated for chemical oxygen demand (COD) and N
166 removal (More details can be found at Rodriguez-Caballero et al., 2015). The N_2O gas
167 emissions were captured by a hood placed in one of the SBRs (Fig. 1 C, D) and were compared
168 between the N_2O gas sensor and a commercial analyser. Simultaneously, a liquid-phase N_2O
169 sensor was applied in the same zone of the SBR as the gas sensor. Temperature in the liquid-
170 phase varied between the range of 16.9 to 17.9 °C.
171
172 *2.2.4. Data acquisition and N_2O emission calculations*
173 2.2.4.1. N_2O Emissions measured by the Gas sensor and Commercial analyser
174 On-line process data from the SBR tank was acquired from the data acquisition system of the
175 WWTP. These values were used to calculate N_2O emissions during the reactor monitoring. The
176 N_2O gas emitted in the aerated phases was calculated using the following equation 2:
177
178 $$N_2O\ gas\ emitted_{(aerated)} = \left[\sum\left(C_{N_2O} \times Q_{gas(aerated)} \times \Delta t\right)\right] \quad (2)$$
179 Where,
180 • N_2O gas emitted $_{(aerated)}$ – N_2O gas emitted during aerated operational times (mg N-N_2O);
181 • C_{N2O} (mg N-N_2O.m^3) = C_{N2O} (ppmv N_2O) × 1/0.08205 atm.L.mol^{-1}.K^{-1} × (28/T(K));

- $Q_{gas(aerated)}$ – gas flow coming out of the reactor during aerated zones ($m^3.d^{-1}$);
- Δt – time interval by which the off-gas concentration was recorded (d);

While during the non-aerated phases the gas emitted was calculated according to the following equations 3 and 4:

$$N_2O\ gas\ emitted\ _{(\text{non}-aerated)} = \left[\left(\sum\left(C_{N_2O} \times Q_{in(\text{non}-aerated)} \times \Delta t\right)\right) \times \left(\frac{A_{Tank}}{A_{hood}}\right)\right] \quad (3)$$

Where,

- N_2O gas emitted$_{(non\text{-}aerated)}$ – N_2O gas emitted during non-aerated operational times (mg N-N_2O);
- A_{hood} – Area of the tank covered by the hood (m^2);
- A_{Tank} – Aeration field size (m^2);
- Q_{in} (L/min) - Flow at which the sample conditioning system pumps gas into the analyser (0.5 L/min);

2.2.4.2. <u>N_2O emissions calculated using liquid-phase measurements</u>

Estimation based on the dissolved N_2O sensor data and the K_La of N_2O was also applied to this full-scale SBR WWTP. During the cycle the reactor was operated with both aerated and non-aerated phases. The aeration was performed using diffused aerators situated near the bottom of the tank. The N_2O gas emitted during aeration was calculated based on the mass transfer coefficient, the input of the air flow, the volume of the reactor, the Henry's coefficient and the concentration of dissolved N_2O through applying Equation 4 (Schulthess and Gujer, 1996):

$$Gas\ emitted_{(aerated)} = H_{N_2O,T_{process}} \times S_{N_2O_{T_{Comp.}}} \times \left[1 - e^{-\frac{K_L a_{N_2O_{T_{Process}}}}{H_{N_2O,T_{process}}} \times \frac{V_R}{Q_{gas}}}\right] \times Q_{gas(aerated)} \times \Delta t \quad (4)$$

Where,

- Gas emitted (aerated) – Emissions of N_2O during the aerated phases (mg N-N_2O);
- $S_{N2O}T_{Comp}$ – Concentration of N_2O in the liquid measured by the N_2O liquid microsensor, after temperature compensation (mg N-N_2O.m^{-3});
- $H_{N2O,}T_{process}$ – Henry`s constant at the process temperature (dimensionless);
- $K_LaN_2OT_{process}$ – N_2O mass transfer coefficient at the process temperature (d^{-1});

For non-aerated periods, a typical K_La for N_2O of $2d^{-1}$ for an anoxic tank was first chosen (Schulthess and Gujer, 1996), and later estimated as described below (equation 8). The rate of N_2O emissions were then calculated using equation 5 (Schulthess and Gujer, 1996):

$$Gas\ emitted_{(non-aerated)} = K_L a_{N_2O(non-aerated)} \times \left(S_{N_2O_{T\_Comp.}} - \frac{C_{N_2O,air}}{H_{N_2O,T_{process}}} \right) \times V_R \times \Delta t \quad (5)$$

Where,

- Gas emitted (non-aerated) – Emissions of N_2O during the non-aerated phases (mg N-N_2O);
- $K_LaN_2OT_{process\ (non\text{-}aerated)}$ – N_2O mass transfer coefficient during non-aerated phases (d^{-1});
- $C_{N2O,}$ air - average concentration of N_2O in the atmosphere of the northern hemisphere, 0.326 mg-N/m^3 according to (Blasing, 2009);

Through rearranging equation 5, the mass transfer coefficient was estimated for non-aerated operational times using the N_2O emissions measured in the gas-phase and in the liquid-phase sensors, as shown in equation 6:

$$K_L a_{N_2O(non-aerated)} = \frac{S_{N_2O_{Gas\ sensor}}}{\left(S_{N_2O_{Liquid\ sensor}} - \frac{C_{N_2O,air}}{H_{N_2O,T_{process}}} \right)} \quad (6)$$

Where,

- $S_{N2O\ Gas\ sensor}$ – Concentration of N_2O in the gas measured by the N_2O gas sensor, after temperature compensation (mg $N\text{-}N_2O.m^{-3}$).
- $S_{N2O\ Liquid\ sensor}$ – Concentration of dissolved N_2O measured by the N_2O liquid microsensor, after temperature compensation (mg $N\text{-}N_2O.m^{-3}$).

This dynamic estimation of K_La during non-aeration conditions was applied during the anoxic phases of WWTP operation, where negative K_La values were assumed to be zero.

The K_La during aeration is related with many factors, including reactor geometry (particularly aerator immersion depth), aeration bubble size, diffuser layout and liquid viscosity (Foley et al., 2010; Gillot et al., 2005). The methodologies used to estimate the K_La during aeration are described in detail in the supplementary information. Briefly, the methodologies applied to assess the K_La during aeration and non-aeration operational times are described below:

- Method 1:
    - (aerated phase) based on the superficial gas velocity of the reactor (Equation S1) as described by Foley et al., (2010);
    - (non-aerated phase) based on a typical K_La for N_2O of $2d^{-1}$ for an anoxic tank (Schulthess and Gujer, 1996);
- Method 2:
    - (aerated phase) based on the superficial gas velocity of the reactor (Equation S1) as described by Foley et al., (2010);
    - (non-aerated phase) based on Equation 6;
- Method 3:
    - (aerated phase) based on the oxygen transfer rate (OTR) of the reactor, assuming pure water (Equation S4);
    - (non-aerated phase) based on a typical K_La for N_2O of $2d^{-1}$ for an anoxic tank (Schulthess and Gujer, 1996);

- Method 4:
    - (aerated phase) based on the oxygen transfer rate (OTR) of the reactor, integrating fouling, salinity and impurity factors in the estimation (Equation S5);
    - (non-aerated phase) based on a typical K_La for N_2O of $2d^{-1}$ for an anoxic tank (Schulthess and Gujer, 1996);
- Method 5:
    - (aerated phase) based on the oxygen transfer rate (OTR) of the reactor integrating fouling, salinity and impurity factors in the estimation (Equation S5);
    - (non-aerated phase) based on Equation 6;

After obtaining the K_La of O_2 at 20ºC for each of the OTR methods (3-5) for the aerated phase, Higbie`s penetration model was applied to calculate the K_La of N_2O applying equation S7 (Foley et al., 2010; Van Hulle et al., 2012) (Equation S7, Supplemental Information). Due to temperature variation along the day, K_La and Henry's constant estimations were corrected for temperature, as described in detail in the Supplemental Information.

3. RESULTS AND DISCUSSION

3.1. Full-scale N_2O sensor calibration

The sensor linearity was tested in three different concentration ranges (0-422.3 ppmv; 0-50 ppmv; 0-10 ppmv) with nitrogen used as dilution gas. The sensor showed high linearity and stability within the ranges tested. No saturation of the signal was observed up to the maximum concentration tested, nor was a decrease in linearity observed at the lower range tested (Supplementary information, Fig. S1). Overall, the sensor was shown to respond linearly over a wide concentration range of N_2O, which is in accordance with the results obtained by Marques et al., (2014) for the lab-scale N_2O gas sensors.

In order to evaluate the sensor and commercial analyser responses at high N_2O levels, as well as the signal saturation of each system, a series of standards were performed at concentrations above 1000 ppmv and compared with GC-ECD. A pure 100% N_2O gas bottle was used and the gas diluted in order to have three gas streams with concentrations of approximately 1000, 2000 and 3000 ppmv of N_2O. The results (Table 1) showed that at the first concentration tested, 1000 ppmv of N_2O, the commercial analyser was already saturated and not able to determine this concentration correctly. The N_2O gas sensor was able to follow the trend and measure the gas stream well at this level. The sensor was also able to correctly measure the N_2O in the gas stream at 2000 ppmv (Table 1). A final gas stream of 3000 ppmv of N_2O was used and showed that the sensor was not able to adequately measure it at this very high level. Further results showed that the sensor was able to measure concentrations up to 2750 ppmv of N_2O (through additional testing), while the commercial analyser was not able to adequately describe any of the high concentrations tested. This validates the applicability of the sensor to measure very high concentrations of N_2O in gas streams.

The temperature dependency of the sensor was tested for the zero current and for selected N_2O concentrations. There was an exponential temperature dependency on the zero current and the tested N_2O concentrations for the sensors. The influence of temperature was well described by an exponential equation and the coefficient of determination had a value of ≥ 0.96 (Fig. 2,A). A similar dependency was also found for the commercially available N_2O microsensors in lab-scale tests for liquid and gas phase measurements (Jenni et al., 2012; Marques et al., 2014).

Since the N_2O sensor measurements depend on temperature, and the air experiences higher temperature fluctuations along the day as compared to the liquid phase, the gas sensor can experience high temperature fluctuations throughout the day. Correct characterization and prediction of the temperature effect on the sensors is essential for their application in full scale systems. A double exponential equation (equation 1) was used to predict the sensor signal, using calibration curves at different temperatures (Fig. 2, B), where only 6 measurements were needed

306 to accurately calibrate the sensor, validating the strategy proposed with the lab-scale gas sensor
307 (Marques et al., 2014). The fitting was performed with 3 different concentrations (0, 25.5 and
308 50.1 ppmv of N_2O) at 2 different temperatures (15.5 and 33.1 °C), though the equation also
309 described well the sensor signal for these 3 concentrations at 2 additional temperatures (22.6
310 and 25.5°C) to validate the temperature dependency. High coefficient of determination values
311 > 0.999 were obtained in this case between the measured and the predicted signal. The
312 maximum difference between the measured and the predicted sensor signal values was 3.0 %.
313 Therefore, the temperature influence on all sensors was effectively predicted using only 6 points
314 of experimental data for calibration. When temperature variations are unavoidable (e.g. at a
315 full-scale WWTP), the correction of the sensor signal should be performed to obtain valid
316 results.
317

318 **3.2. Comparing the N_2O gas sensor with the online gas analyser at full-scale**

319 The sensor was attached to the hood and placed in the SBR at the WWTP. The N_2O gas
320 emissions were collected and characterized during 4 days. The sensor signal was corrected for
321 the temperature variations using equation 1. Fig. 3 shows the results obtained with the sensor
322 and the commercial N_2O gas analyser. The sensor was able to describe very well the trend in
323 the emissions when compared with the commercial analyser. Due to saturation of the
324 commercial analyser at N_2O concentrations above 500 ppmv (as indicated by the manufacturer),
325 the higher emission peaks were in fact much better described by the full-scale gas sensor (Fig.
326 3). This shows that the wide detection range of the microelectrode can result in improved ability
327 to estimate N_2O emissions, and that N_2O peaks measured by conventional analysers may be
328 underestimating the true emissions in cases where the concentration exceeds their upper
329 detection limit (in the case of this study, 500 ppmv). Rodriguez-Caballero et al., (2014) also
330 reported the importance of correctly characterizing peak emissions in their study, where even
331 isolated peak emissions had a significant impact on the global emissions of a WWTP.

The emissions from the full-scale SBR were calculated using equation 2 for aerobic phases and equation 3 for anoxic phases, where the phases were differentiated based on the measured DO concentration in the liquid after aeration commenced or ceased. When comparing the overall N_2O emissions between the sensor and the commercial analyser, there was a difference of 14.1% between both (Table 2). As shown in Fig. 3, this difference is mainly due to the underestimated N_2O peaks in the case of the commercial analyser, which had already exceeded its saturation signal. This difference decreases significantly when analysing the emissions as assessed by the sensor and commercial analyser below 500 ppmv, where the difference was only 2.0 %. Thus, at levels below 500 ppmv, the sensor and commercial analyser achieved highly comparable results, supporting the applicability of either methodology in this concentration range. Further, peak emissions should be correctly characterized because the N_2O peak emission events can significantly increase the overall N_2O emission factor of a WWTP. The high variability of peak emissions (very high and low), under aerated and non-aerated conditions, varying DO, temperature and aeration flow rates, validate the use of the gas sensor to accurately quantify the N_2O emissions when subjected to the variable conditions present in a WWTP. Overall, the results validate the use of the gas sensor to measure N_2O emissions in a WWTP, even achieving a wider range of emission rates than currently achieved by a commercial analyser.

The anoxic emissions measured with both techniques were very similar (Table 2a, 2b). When comparing the total emissions between the aerobic and anoxic phases, the aerobic phase was the main contributor with over 96.1% of the total emissions. These results agree with the studies of Ahn et al., 2010; Ye et al., 2014, where the aerobic phase contributes with higher N_2O emissions as compared with the anoxic due to the higher rate of N_2O production and stripping during aeration.

3.3. N_2O gas emission estimation through dissolved N_2O measurements

The total emissions were calculated for the aerobic and anoxic periods using the dissolved N_2O sensor data, with five different approaches to estimate the K_La of N_2O during aeration. The first approach consisted on using the superficial gas velocity in the liquid (Method 1) resulting in a difference of 19.5 % between the calculated emissions based on dissolved N_2O data and the measured emissions with the N_2O gas sensor (

). During the four days of monitoring, a higher difference was observed in the emissions predicted by the liquid sensor for the first 2 days (period_a: 32.7%), as compared to the last 2 days (period_b: 4.4%), when comparing the results to the gas sensor emissions (

3 – Method 1). This difference was likely due to the accumulation of particles on the liquid sensor observed during the monitoring of period_a (first 2 days), while during period_b (last 2 days) the sensor was cleaned once per day.

The second approach consisted of calculating the K_La based on the OTR (Method 3). A difference of 12.9 % between the total emissions measured by the gas sensor and the calculated emissions based on dissolved N_2O data was found (

– Method 3). As observed in the previous approach, the difference in the emissions was higher during period_a as compared to period_b. To increase the applicability of the model equation using the Method 3 estimation methodology, the main factors affecting liquid-gas mass transfer in wastewater systems were taken into account, including salinity (β), impurities (α) and fouling (F). The total estimated emissions obtained with this approach (Method 4) were closer (8.2%) to the emissions measured by the N_2O gas sensor (

– Method 4).

When evaluating the aerobic emissions, considering each methodology, higher agreement with the gas sensor emissions was achieved for period_b, with differences of 4.4, 11.4 and 16.1 % for Method 1, Method 3 and Method 4, respectively. While for period_a the differences between the emissions measured by the gas sensor with each methodology (Method 1, Method 3 and Method 4) were 32.7, 26.9 and 23.0 %, respectively. Furthermore, the total predicted emissions in the anoxic phase were substantially higher as compared with the ones measured by the gas sensor. This indicates that the emissions of the non-aerated phases were overestimated, and this overestimation compensated somewhat for the underestimated aerobic emissions during period_a. This overestimation in the anoxic phase can be related with the use of a typical K_La for N_2O of $2d^{-1}$ for anoxic tanks (Method 1, 3 and 4), which was originally determined for continuous activated sludge processes (Schulthess and Gujer, 1996). This estimation of K_La was thus not applicable to the present WWTP, a full-scale SBR, and required reassessment to avoid overestimation of the N_2O emissions. To correct this, the K_La for anoxic zones was calculated based on the dynamic emissions measured by the N_2O gas and liquid sensors (Equation 6, Method 2 and 5). The average anoxic K_La throughout the experimental period was 0.39 d^{-1}, five times smaller than the previously applied value. The SBR configuration of the studied WWTP clearly influenced this mass transfer coefficient, as there was lower turbulence in the SBR as compared to continuous-flow WWTPs. Dynamic estimation of the anoxic K_La increased the confidence of the model equations to estimate the emissions calculated using dissolved N_2O data, particularly for the Method 5.

A comparison between the dynamic N_2O emissions as assessed by the gas sensor and estimated via the liquid sensor is shown in Figure 4 for 3 typical cycles during the monitoring of the plant (period_b). By applying equation 6, the anoxic kLa was corrected according with the emission measure by the N_2O gas sensor (Method 2 and 5). The predicted emissions based on the dissolved N_2O data using estimation Method 5 agreed very well with the emissions captured by the hood and measured with the N_2O gas sensor. The prediction of N_2O emissions during

period_a show higher deviation as compared to the gas-phase analysis (Fig. S2, Supplementary information), highlighting the importance of sensor cleaning. It is also clear from Figure 4 that the N_2O emissions were mainly attributed to aerobic production mechanisms rather than anoxic production and subsequent aerobic stripping. Indeed, while the dissolved N_2O concentrations were initially high anoxically, they were gradually reduced along the anoxic and settling phases, contributing little to the total N_2O emissions during this time period due to the very low anoxic K_La. Aerobically, the initial N_2O emissions were consistently negligible, revealing near-complete denitrification during the previous anoxic and settle/decant phases, with minimal carryover of the anoxically produced N_2O to the subsequent aerobic phase where it would be more readily emitted. These results highlight that estimation of both the aerobic and anoxic K_La can be useful to both quantify the total N_2O emissions using dissolved N_2O measurements and identify operational factors that lead to these emissions.

The total emissions obtained from the SBR analysed in this study were 48.6 and 41.8 gN-N_2O/kg N-NH_4^+ removed for the N_2O gas sensor and the online commercial analyser, respectively, during the total measurement period. Underestimation of the emissions was evident when comparing these two methodologies due to the high peak emissions that could not be effectively quantified by the commercial analyser. The total estimated emission values obtained using the dissolved N_2O measurements were 33.3 and 38.8 gN-N_2O/kg N-NH_4^+ for the methodologies using Method 2 and Method 5, respectively. However, when taking into account only period_b, the emissions of the liquid sensor (Method 2) underestimated the gas sensor emissions by 13.0 %, while the liquid sensor (Method 5) emissions agreed within 98.7 %. The estimation of the emissions using the OTR-based method, where both the aerobic and anoxic K_La are calculated, was shown to be a reasonable means of providing a good estimation of the total N_2O emissions, where regular cleaning of the sensor can increase the validity of these estimations.

3.4 Comparison of N_2O monitoring methodologies

The results of this study showed that the gas sensor is advantageous over conventional online gas analysers due to its higher measurement range. The gas sensor signal has a very low drift over time and by applying the drift correction, the sensor could be continuously used without performing additional calibration during several weeks, which is comparable to conventional analysers. The additional step required for the application of N_2O gas sensors as compared to conventional gas analysers is the calibration step at different temperatures. Nevertheless, this study showed that this can be effectively achieved with 6 experimental measurements, minimising labour. The gas sensor does not require regular cleaning, although it has a limited lifetime (~6 months). Unlike conventional analysers, however, the gas sensor does not require pre-conditioning of the gas sample prior to measurement. This increases maintenance requirements to the measurement system, as regular maintenance checks are required in conventional analysers. Thus, both systems require occasional maintenance and/or replacement of parts.

The dissolved N_2O sensor signal is also very stable over time, and, as suggested by the manufacturer (Unisense Environment, Denmark), requires only a bimonthly calibration, which takes around 10 minutes and does not involve measurements at different temperatures. Regarding the cleaning of the sensor, we observed an improvement of the signal if the sensor was cleaned on a daily basis. However, an improved version of this sensor to be used for full-scale measurements is now commercially available, and the manufacturer claims that no regular cleaning is needed (Unisense Environment, Denmark). The liquid and gas-phase N_2O sensors have a similar lifetime. In this study it was found that emissions were effectively estimated within a reasonable error based on dissolved N_2O sensor signals.

For highest rigour, the simultaneous utilisation of an N_2O sensor in both the gas and liquid phases is recommended, as it also enables estimation of the relative importance of the aerobic or anoxic N_2O production mechanisms. Furthermore, both signals can be measured using only

461 one multimeter controller, decreasing total cost of the equipment. Overall, this work shows that
462 the analytical methodology employed to assess N_2O emissions can have a significant influence
463 on the N_2O emission factor obtained for WWTPs. We recommend that this new methodology
464 also be applied to assess N_2O emissions at other full-scale WWTPs.
465
466 **4. CONCLUSIONS**
467 The main conclusions of this work are summarised below:
468 • The N_2O Clark-type full-scale gas sensor proved to be a reliable alternative to standard
469 methods for online detection of N_2O emissions in the gas phase of WWTPs.
470 • The sensor was linear at both low and high ranges of N_2O concentrations, reaching an
471 upper detection limit of 2750 ppmv N_2O. Routine calibrations should be performed, and
472 the temperature influence on the sensor signal must be adequately predicted.
473 • Emissions were successfully described by the gas sensor, being even more accurate than
474 the values given by the commercial analyser at N_2O concentrations above 500 ppmv.
475 Total N_2O emissions were underestimated by 14.0 % by the commercial analyser in this
476 study.
477 • The two proposed methodologies to estimate N_2O emissions using dissolved N_2O
478 measurements performed by a full-scale liquid N_2O sensor with best results agreed by
479 98.7% (Method 5) or 87.0 % (Method 2) with the emissions measured by the gas sensor.
480 This is the first study showing a reliable estimation of gas emissions based on dissolved
481 N_2O online data in a full-scale wastewater treatment facility.
482 • This proposed methodology has the added advantage of simultaneously analysing the
483 N_2O dynamics in the liquid and gaseous phases, in only one experimental setup, and
484 can in this way contribute to improve the characterisation of the N_2O emission
485 mechanism in the WWTP.
486

Acknowledgements

This study was funded by the Spanish Government (MINECO) (CTM 2011-27163 and CTM2015-66892-R), European Commission (FP7-PEOPLE-2011-CIG 303946) and the Portuguese Fundação para a Ciência e Tecnologia (PTDC/AAC-AMB/12058/2010, UID/Multi/04378/2013, PhD grant SFRH/BD/74515/2010). Spanish and Portuguese Governments are also acknowledged for Acciones Integradas (PRI-AIBPT-2011-1232) and Luso-Espanhola action E-61/12. M. The European Commission is also acknowledged through COST action ES1202 (Water 2020). M. Pijuan acknowledges the Ramon y Cajal Research fellowship (RYC-2009-04959) from the Spanish Government. We thank Dr. Mikkel Holmen Andersen (Unisense Environment, Denmark) for providing the sensors and helpful comments.

References

Aboobakar, A., Cartmell, E., Stephenson, T., Jones, M., Vale, P., Dotro, G., 2013. Nitrous oxide emissions and dissolved oxygen profiling in a full-scale nitrifying activated sludge treatment plant. Water Res. 47, 524–34.

Ahn, J.H., Kim, S., Park, H., Rahm, B., Pagilla, K., Chandran, K., 2010. N2O emissions from activated sludge processes, 2008-2009: results of a national monitoring survey in the United States. Environ. Sci. Technol. 44, 4505–4511.

Blasing, T.J., 2009. Recent Greenhouse Gas Concentrations. [WWW Document]. URL http://digital.library.unt.edu/ark:/67531/metadc11963/

Daelman, M.R.J., De Baets, B., van Loosdrecht, M.C.M., Volcke, E.I.P., 2013. Influence of sampling strategies on the estimated nitrous oxide emission from wastewater treatment plants. Water Res. 47, 3120–3130.

Daelman, M.R.J., van Voorthuizen, E.M., van Dongen, L.G.J.M., Volcke, E.I.P., van Loosdrecht, M.C.M., 2013. Methane and nitrous oxide emissions from municipal wastewater treatment - results from a long-term study. Water Sci. Technol. 67, 2350–5.

Daelman, M.R.J., van Voorthuizen, E.M., van Dongen, U.G.J.M., Volcke, E.I.P., van Loosdrecht, M.C.M., 2015. Seasonal and diurnal variability of N2O emissions from a full-scale municipal wastewater treatment plant. Sci. Total Environ. 536, 1–11.

De Haas, D., Hartley, K., 2004. Greenhouse gas emission from BNR plants-do we have the

517 right focus?. In: Paper Presented at the Proceedings of EPA Workshop: Sewage
518 Management, Risk Assessment & Triple Bottom Line. Cairns, Australia, 5-7 April 2004

519 Ferrell, R.T., Himmelblau, D.M., 1967. Diffusion coefficients of nitrogen and oxygen in water.
520 J. Chem. Eng. Data 12, 111–115.

521 Foley, J., de Haas, D., Yuan, Z., Lant, P., 2010. Nitrous oxide generation in full-scale biological
522 nutrient removal wastewater treatment plants. Water Res. 44, 831–44.

523 Gillot, S., Capela-Marsal, S., Roustan, M., Héduit, a., 2005. Predicting oxygen transfer of fine
524 bubble diffused aeration systems - Model issued from dimensional analysis. Water Res.
525 39, 1379–1387.

526 IPCC, Stocker, T.F., Qin, D., Plattner, G.-K., Tignor, M.M.B., Allen, S.K., Boschung, J.,
527 Nauels, A., Xia, Y., Bex, V., Midgley, P.M., 2013. Climate Change 2013 - The Physical
528 Science Basis, Intergovernmental Panel on Climate Change.

529 Jenni, S., Mohn, J., Emmenegger, L., Udert, K.M., 2012. Temperature dependence and
530 interferences of NO and N_2O microelectrodes used in wastewater treatment. Environ. Sci.
531 Technol. 46, 2257–66.

532 Kampschreur, M.J., Temmink, H., Kleerebezem, R., Jetten, M.S.M., van Loosdrecht, M.C.M.,
533 2009. Nitrous oxide emission during wastewater treatment. Water Res. 43, 4093–103.

534 Law, Y., Ye, L., Pan, Y., Yuan, Z., 2012. Nitrous oxide emissions from wastewater treatment
535 processes. Philos. Trans. R. Soc. B Biol. Sci. 367, 1265–1277.

536 Mampaey K.E., van Dongen U.G.J.M., van Loosdrecht M.C.M., Volcke E.I.P., 2015. Novel
537 method for online monitoring of dissolved N2O concentrations based on gas phase
538 measurements. Environmental Technology, 36(13), 1680-1690.

539 Marques, R., Oehmen, A., Pijuan, M., 2014. Novel Microelectrode-Based Online System for
540 Monitoring N 2 O Gas Emissions during Wastewater Treatment. Environ. Sci. Technol.
541 48, 12816–12823.

542 Metcalf & Eddy, I., 2003. Wastewater engineering: Treatment and Reuse, 4th ed, McGraw-Hill
543 Education. New York.

544 Rodriguez-Caballero, a., Aymerich, I., Marques, R., Poch, M., Pijuan, M., 2015. Minimizing
545 N2O emissions and carbon footprint on a full-scale activated sludge sequencing batch
546 reactor. Water Res. 71, 1–10.

547 Rodriguez-caballero, A., Aymerich, I., Poch, M., Pijuan, M., 2014. Evaluation of process
548 conditions triggering emissions of green-house gases from a biological wastewater
549 treatment system. Sci. Total Environ. 493, 384–391.

550 Schulthess, R., Gujer, W., 1996. Release of nitrous oxide (N 2 O) from denitrifying activated
551 sludge: Verification and application of a mathematical model. Water Res. 30, 521–530.

552 Stenstrom, M.K., Gilbert, R.G., 1981. Effects of alpha, beta and theta factor upon the design,

553 specification and operation of aeration systems. Water Res. 15, 643–654.

554 Tamimi, A., Rinker, E.B., Sandall, O.C., 1994. Diffusion Coefficients for Hydrogen Sulfide,
555 Carbon Dioxide, and Nitrous Oxide in Water over the Temperature Range 293-368 K. J.
556 Chem. Eng. Data 39, 330.

557 Unisense, 2014. Nitrous Oxide Sensor User Manual. Unisense, Aarhus.

558 Van Hulle, S.W.H., Callens, J., Mampaey, K.E., van Loosdrecht, M.C.M., Volcke, E.I.P., 2012.
559 O and NO emissions during autotrophic nitrogen removal in a granular sludge reactor – a
560 simulation study. Environ. Technol. 1–10.

561 Ye, L., Ni, B.J., Law, Y., Byers, C., Yuan, Z., 2014. A novel methodology to quantify nitrous
562 oxide emissions from full-scale wastewater treatment systems with surface aerators. Water
563 Res. 48, 257–268.

564

565

List of Figures:

Fig. 1– A– Full-scale N_2O gas sensor and controller box; B – Full-scale dissolved N_2O sensor and controller box; C – Close-up of the gas sensor placed in the sampling hood; D – Sampling hood placed in the full-scale activated sludge SBR.

Fig. 2 – A - Exponential variation of sensor signal with three different N_2O gas mixtures (● 0 ppmv, ▲25.5 ppmv, ■ 50.1 ppmv) as a function of temperature at a range of 15 to 35 °C; B - Measured (open symbols) and predicted (close symbols) signal values for concentrations of 0 (●,○), 25.5 (▲,Δ), and 50.1 (■,□) ppmv of N_2O for the sensor. Prediction equation for the sensor was S_{N2O} (T,C) = $1238.3e^{0.002T}+1.638Ce^{0.009T}$.

Fig. 3 – N_2O emissions over a 4 day monitoring period at the full scale SBR with the gas sensor (green line) and the commercial analyser (blue line).

Fig. 4 – Typical SBR profile at La Roca del Vallès WWTP of N_2O gas emissions (blue dashed line), liquid N_2O concentration (orange line), DO concentration (grey line) and N_2O dissolved emitted predicted (black dashed line) (KLa_OTR_III – period_b). A – aerobic phase, B – anoxic phase and C-settling and decant phase.

List of Tables:

Table 4– Emissions of N_2O per ammonia removal measured by the gas sensor, commercial analyser, and liquid phase-sensor.

Table 1 – Comparison between the gas sensor, commercial analyser and GC-ECD between 3 different mixtures with approximate concentrations of 1000, 2000 and 3000 ppmv of N_2O.

Table 2 – Comparison between the total emissions and emissions limited up to 500 ppmv between the N_2O gas sensor and the commercial analyser.

Table 3 – Emission comparison between N_2O measured with the Gas sensor, Commercial analyser and the methodologies used to estimate the gas emissions using the N_2O liquid sensor. The difference between the N_2O measured with the gas sensor and the respective methodology used to estimate the N_2O emission using the liquid sensor is shown in brackets.

Fig. 1– A– Full-scale N_2O gas sensor and controller box; B – Full-scale dissolved N_2O sensor and controller box; C – Close-up of the gas sensor placed in the sampling hood; D – Sampling hood placed in the full-scale activated sludge SBR.

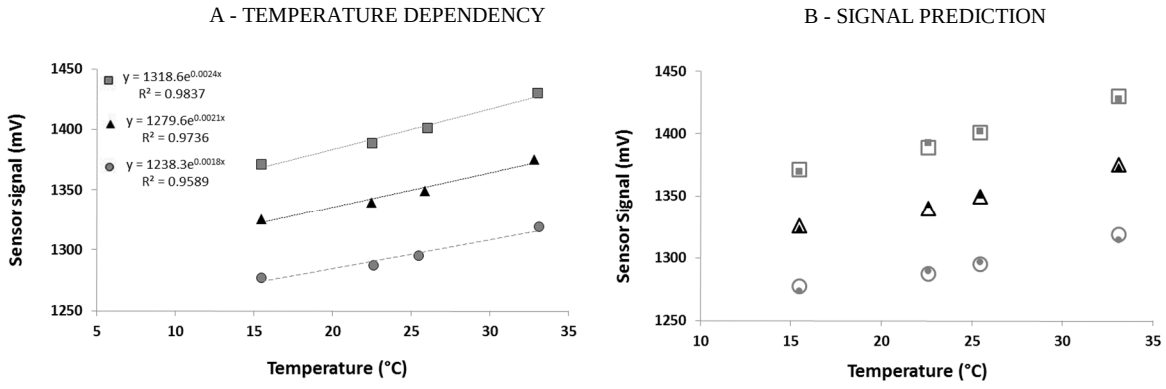

Fig. 2 – A - Exponential variation of sensor signal with three different N_2O gas mixtures (● 0 ppmv, ▲25.5 ppmv, ■ 50.1 ppmv) as a function of temperature at a range of 15 to 35 °C; B - Measured (open symbols) and predicted (close symbols) signal values for concentrations of 0 (●,○), 25.5 (▲,Δ), and 50.1 (■,□) ppmv of N_2O for the sensor. Prediction equation for the sensor was S_{N2O} (T,C) = $1238.3e^{0.002T}+1.638Ce^{0.009T}$.

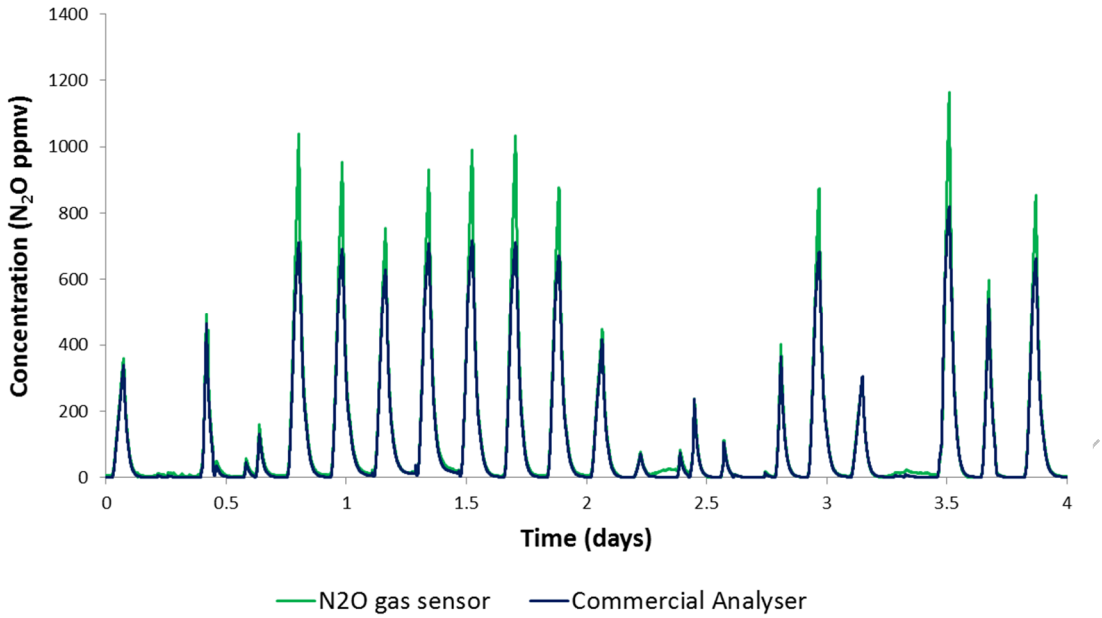

612

613 **Fig. 3 – N_2O emissions over a 4 day monitoring period at the full scale SBR with the gas**
614 **sensor (green line) and the commercial analyser (blue line).**

615

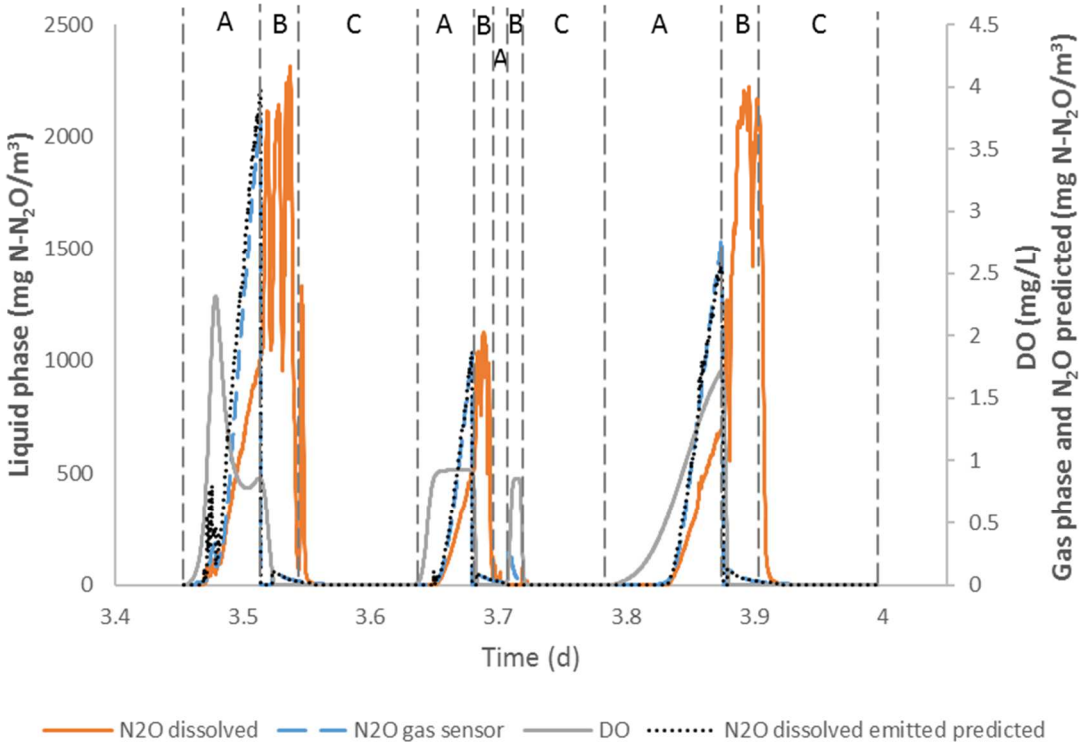

616

617 **Fig. 4 –** Typical SBR profile at La Roca del Vallès WWTP of N_2O gas emissions (blue dashed
618 line), liquid N_2O concentration (orange line), DO concentration (grey line) and N_2O dissolved
619 emitted predicted (black dashed line) (Method 5 – period_b). A – aerobic phase, B – anoxic
620 phase and C-settling and decant phase.

621

Table 1 – Comparison between the gas sensor, commercial analyser and GC-ECD between 3 different mixtures with approximate concentrations of 1000, 2000 and 3000 ppmv of N_2O.

	Gas Sensor (ppmv)			Commercial Analyser (ppmv)			GC-ECD (ppmv)		
	1000	**2000**	**3000**	**1000**	**2000**	**3000**	**1000**	**2000**	**3000**
Average	1072	2029	2829*	774	946	NT	1036	2115	3037
STD (%)	0.05	0.32	0.01	0.06	0.66	NT	8.81	0.81	0.06

NT- concentration not tested with this equipment; * - saturation of the N_2O gas sensor reached.

Table 2 – Comparison between the total emissions and emissions limited up to 500 ppmv between the N_2O gas sensor and the commercial analyser.

Total emissions	**Gas Sensor (KgN-N_2O)**	**Commercial analyser (KgN-N_2O)**	**Difference (%)**	
Total emissions	19.69	16.91	14.11	a
Aerobic	18.93	16.27	14.04	
Anoxic	0.76	0.64	15.82	
Emissions (<500 ppmv)	**Gas Sensor (KgN-N_2O)**	**Commercial analyser (KgN-N_2O)**	**Difference (%)**	
Total emissions	8.42	7.71	2.04	b
Aerobic	7.84	7.68	2.03	
Anoxic	0.58	0.50	13.88	

Table 3 – Emission comparison between N_2O measured with the Gas sensor, Commercial analyser and the methodologies used to estimate the gas emissions using the N_2O liquid sensor. The difference between the N_2O measured with the gas sensor and the respective methodology used to estimate the N_2O emission using the liquid sensor is shown in brackets.

Emissions	Gas sensor	Commercial analyser	Liquid sensor (Method 1)	Liquid sensor (Method 2)	Liquid sensor (Method 3)	Liquid sensor (Method 4)	Liquid sensor (Method 5)
	Emissions	Emissions	Emissions	Emissions with K_La (non-aerobic) estimated)	Emissions (pure water)	Emissions (with α, β and F)	Emissions (with α, β, F and K_La (non-aerobic) estimated)
	(KgN-N_2O)	(KgN-N_2O)	(KgN-N_2O)	(KgN-N_2O)	(KgN-N_2O)	(KgN-N_2O)	(KgN-N_2O)
Total emissions	19.69	16.91	15.85 (19.5)	13.48 (31.5)	17.15 (12.9)	18.07 (8.2)	15.70 (20.2)
Aerobic	18.93	16.27	12.92 (31.7)	12.92 (31.7)	14.22 (24.8)	15.14 (20.0)	15.14 (20.0)
Anoxic	0.76	0.64	2.93	0.56	2.93	2.93	0.56
Period_a	12.75	10.81	8.58 (32.7)	7.45 (41.6)	9.32 (26.9)	9.81 (23.0)	8.67 (31.9)
Period_a (Aerobic)	12.28	10.40	7.09 (42.2)	7.09 (42.2)	7.83 (36.2)	8.32 (32.2)	8.32 (32.2)
Period_a (Anoxic)	0.47	0.41	1.49	0.35	1.49	1.49	0.35
Period_b	6.94	6.10	7.26 (4.4)	6.04 (13.0)	7.83 (11.4)	8.26 (16.1)	7.03 (1.3)
Period_b (Aerobic)	6.65	5.87	5.83 (12.4)	5.83 (12.4)	6.39 (3.9)	6.82 (2.4)	6.82 (2.4)
Period_b (Anoxic)	0.29	0.23	1.44	0.21	1.44	1.44	0.21

Table 4– Emissions of N_2O per ammonia removal measured by the gas sensor, commercial analyser, and liquid phase-sensor.

Emissions (g N-N_2O/kg NH_4)	Total	Period_a	Period_b
Gas sensor	48.6	55.7	39.5
Commercial analyser	41.8	47.2	34.7
Liquid sensor (Method 2)	33.3	32.5	34.3
Liquid sensor (Method 5)	38.8	37.9	40.0

665

666